Supplementary Material

L5F	Mutation not performed – out of range
L5F, G476S	Mutation not performed – out of range
L5F, D614G	Mutation not performed – out of range
L5F, D614G, D839Y	Mutation not performed – out of range
L5X	Mutation not performed – out of range
L5X, D614G	Mutation not performed – out of range
L8V	Mutation not performed – out of range
L8V, P1263L	Mutation not performed – out of range
L8W, D614G	Mutation not performed – out of range
L8X, D614G	Mutation not performed – out of range
H49Q	Mutation performed
H49X, D614X	Mutation not performed – nonsense mutation
H49X, D614G	Mutation not performed – nonsense mutation
H49Y	Mutation performed
H49Y, D614G	Mutation performed
Y145H, D614G	Mutation performed
Q239H, D614G	Mutation performed
Q239K, D614G	Mutation performed
Q239R, D614G	Mutation performed
Q239X, D614G	Mutation not performed – nonsense mutation
V367F	Mutation performed
V367X	Mutation not performed – nonsense mutation
V367F, D614G	Mutation performed
G476S	Mutation performed
G476S, D614G	Mutation performed
V483A	Mutation performed
V483F, D614G	Mutation performed
V483I	Mutation performed
V483X, D614G	Mutation not performed – nonsense mutation
D614G	Mutation performed
A831S	Mutation performed
D614G, A831V	Mutation performed
D614G, D839E	Mutation performed

D839N	Mutation performed
D839X	Mutation not performed – nonsense mutation
D614X, D839X	Mutation not performed – nonsense mutation
D614G, D839Y	Mutation performed
D936H	Mutation performed
D936X	Mutation not performed – nonsense mutation
D936Y	Mutation performed
D614G, P1263L	Mutation not performed – out of range
P1263L	Mutation not performed – out of range
D614G, P1263X	Mutation not performed – out of range

Table S1. Amino acid mutations associated to 13741 sequences of the Spike protein available on May 08 in COVID-19 Viral Genome Analysis Pipeline, enabled by data from GISAID.

Random 1	L1145F, A1080F, H1088Q
Random 2	I402A
Random 3	F906N, G1035V
Random 4	L865E, N234Y
Random 5	G103H, T881L
Random 6	N74D, L242V, S161W, L335M
Random 7	R1019K, Y636F, L611A, G889I
Random 8	D820R, V213N
Random 9	G971H, G683I, V635P
Random 10	L223M, Q690V, V736C
Random 11	N343C, D290Q, I472P
Random 12	Y741F, S929P
Random 13	F888M
Random 14	N149I, L270S
Random 15	P412H
Random 16	Y365I
Random 17	N17W
Random 18	V1060F, P600L
Random 19	P57Q, V915W, L84W
Random 20	F797A, Q1010W, D1118N
Random 21	T167E
Random 22	Q1005L, A771L
Random 23	T240Y, V656I, F592T, L828K
Random 24	K113Q, Q506H, M697F
Random 25	T599E, E281V, W1102M, N331Y
Random 26	L118C, P330K, F55P
Random 27	I850L, S673R, F1052H, L216P
Random 28	Q414S, P1140Q
Random 29	D737S, W353E, F175R
Random 30	R328G, V512G, E96M, K557H

Table S2. Random mutants accumulating from one to four mutations.

Variant	$\Delta S_{vib\ (open)} - \Delta S_{vib\ (close)}$	Predicted Occupancy		
		Open state	Closed State	Difference (Open – Closed)
Q14H	0.345	25.836%	74.164%	-48.328%
N61P	0.324	25.835%	74.165%	-48.330%
K417I	0.467	25.806%	74.194%	-48.389%
P491H	0.374	25.804%	74.196%	-48.391%
R355Y	-0.632	25.772%	74.228%	-48.456%
Q14F	0.350	25.765%	74.235%	-48.470%
Y369N	0.379	25.731%	74.269%	-48.538%
K417C	0.500	25.725%	74.275%	-48.549%
Q409A	0.403	25.719%	74.281%	-48.562%
F486M	0.310	25.658%	74.342%	-48.684%
R355W	-0.541	25.648%	74.352%	-48.705%
I231P	-0.566	25.622%	74.378%	-48.756%
G416S	0.331	25.503%	74.497%	-48.994%
K417M	0.310	25.467%	74.533%	-49.066%
G416N	0.306	25.319%	74.681%	-49.362%
P230Y	-0.547	25.248%	74.752%	-49.505%
Y489M	0.422	25.168%	74.832%	-49.663%
D111W	-0.547	25.162%	74.838%	-49.677%
F464L	-0.575	25.030%	74.970%	-49.941%
E465W	0.361	24.977%	75.023%	-50.046%
E465K	0.322	24.896%	75.104%	-50.208%
E465Y	0.391	24.798%	75.202%	-50.405%
D111F	-0.656	24.782%	75.218%	-50.436%
Y369V	0.382	24.711%	75.289%	-50.578%
L368N	0.339	24.650%	75.350%	-50.700%
L368G	0.330	24.581%	75.419%	-50.838%
P230D	-0.683	24.515%	75.485%	-50.969%
L368S	0.337	24.336%	75.664%	-51.329%
L368C	0.358	24.173%	75.827%	-51.654%
S469W	-0.523	23.995%	76.005%	-52.011%
L368A	0.383	23.954%	76.046%	-52.091%
L368P	0.331	23.829%	76.171%	-52.342%
Y369E	0.501	23.744%	76.256%	-52.513%
E465A	0.360	23.694%	76.306%	-52.612%
E465S	0.336	23.051%	76.949%	-53.897%
G404Y	0.414	22.941%	77.059%	-54.117%
V503D	0.303	22.614%	77.386%	-54.773%

G404H	0.341	22.321%	77.679%	-55.359%
R403N	0.331	21.822%	78.178%	-56.356%
R403P	0.308	21.716%	78.284%	-56.568%
N394K	-0.524	21.586%	78.414%	-56.828%
G404N	0.411	21.544%	78.456%	-56.911%
Y421G	0.455	14.552%	85.448%	-70.896%
G232E	-0.707	11.578%	88.422%	-76.844%
G232S	-0.686	8.996%	91.004%	-82.008%
G232V	-0.713	5.508%	94.492%	-88.983%
G232P	-0.647	5.042%	94.958%	-89.917%
G232C	-0.664	3.065%	96.935%	-93.870%
G232M	-0.609	3.033%	96.967%	-93.935%
G232Q	-0.688	2.773%	97.227%	-94.454%
G232T	-0.602	1.350%	98.650%	-97.300%

Table S3. Putative mutations and associated $\Delta\Delta S_{vib}$ (in units of $J.K^{-1}$) and predicted occupancies for the open and closed states for the 64 mutants with $\Delta\Delta S_{vib}>0.3$ and the 20 mutants with lowest $\Delta\Delta S_{vib}$ scores.

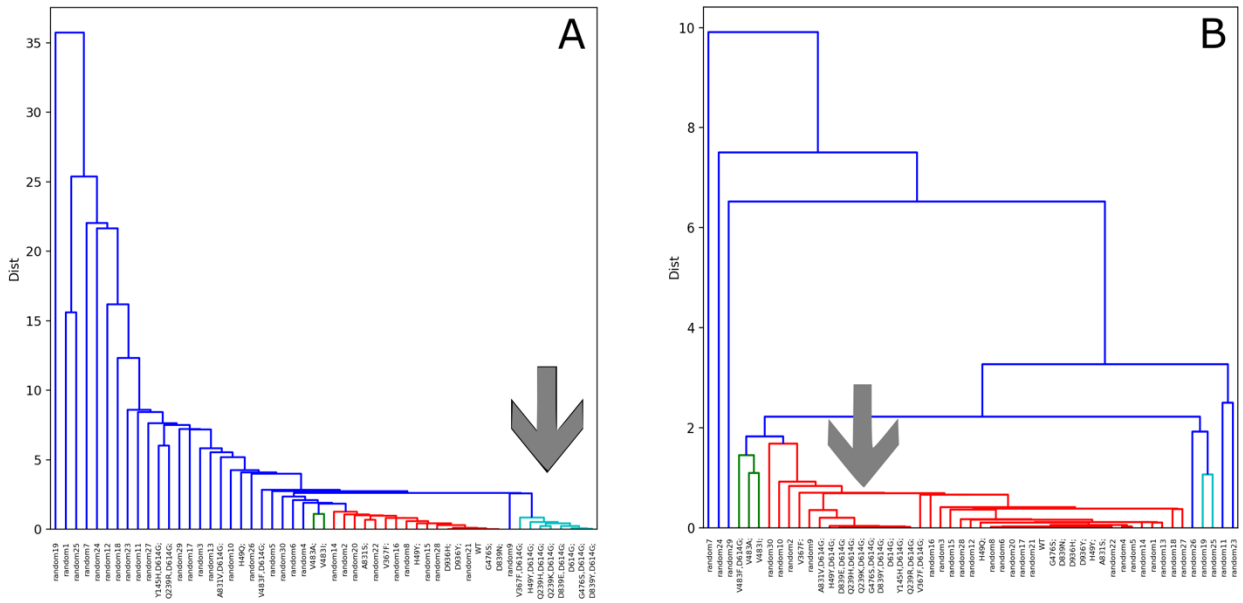

Figure S1. Dynamic Signature clustering between WT, 22 mutants observed in nature and 30 random mutants designed, both for the full structure (A) and only for the RBD (B). The grey arrow highlights the clusters containing most of the mutants that have the mutation D614G.

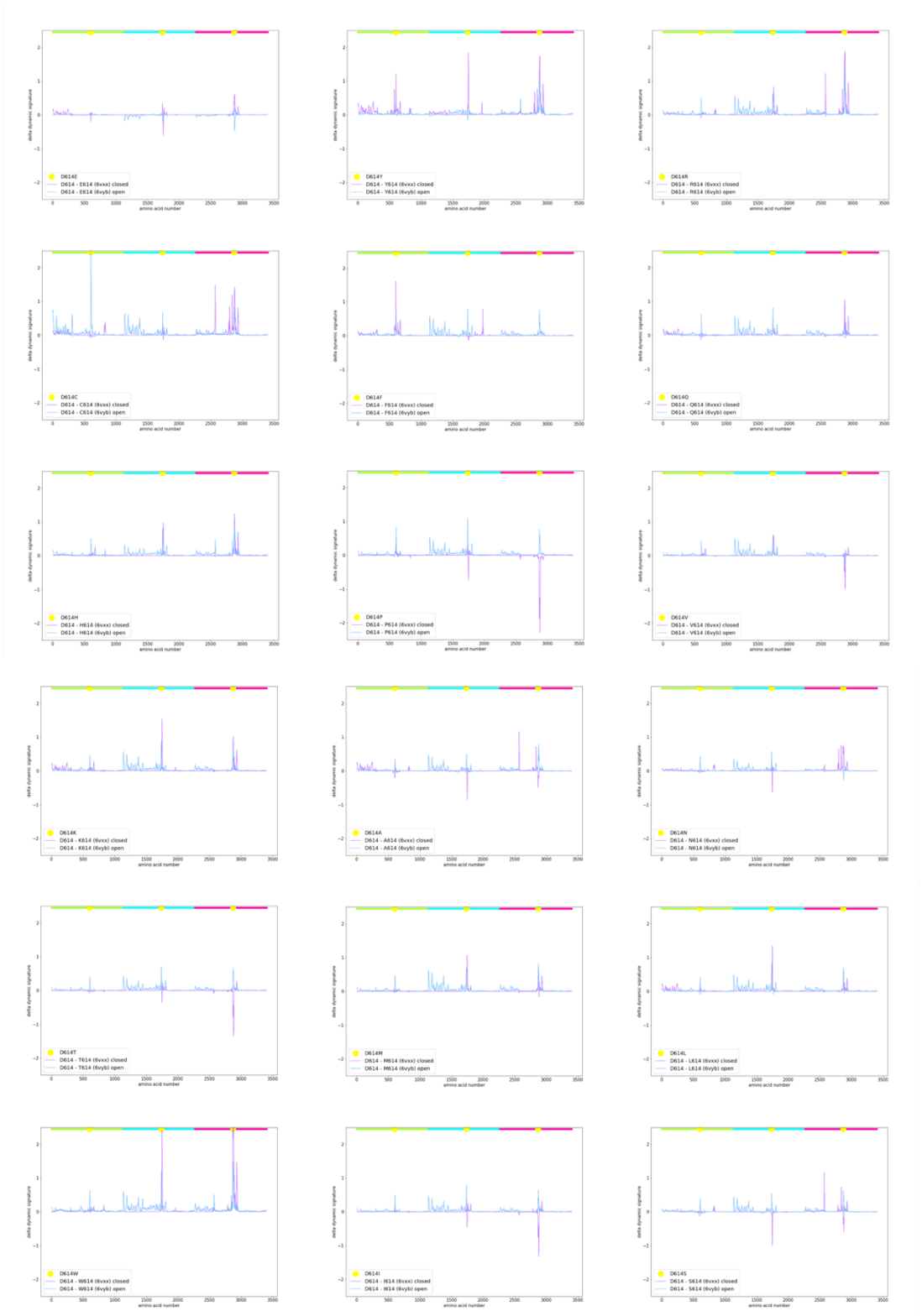

Figure S2. Effects on the Dynamic Signatures of the mutation from D614 to each one of the other 18 possible residues.

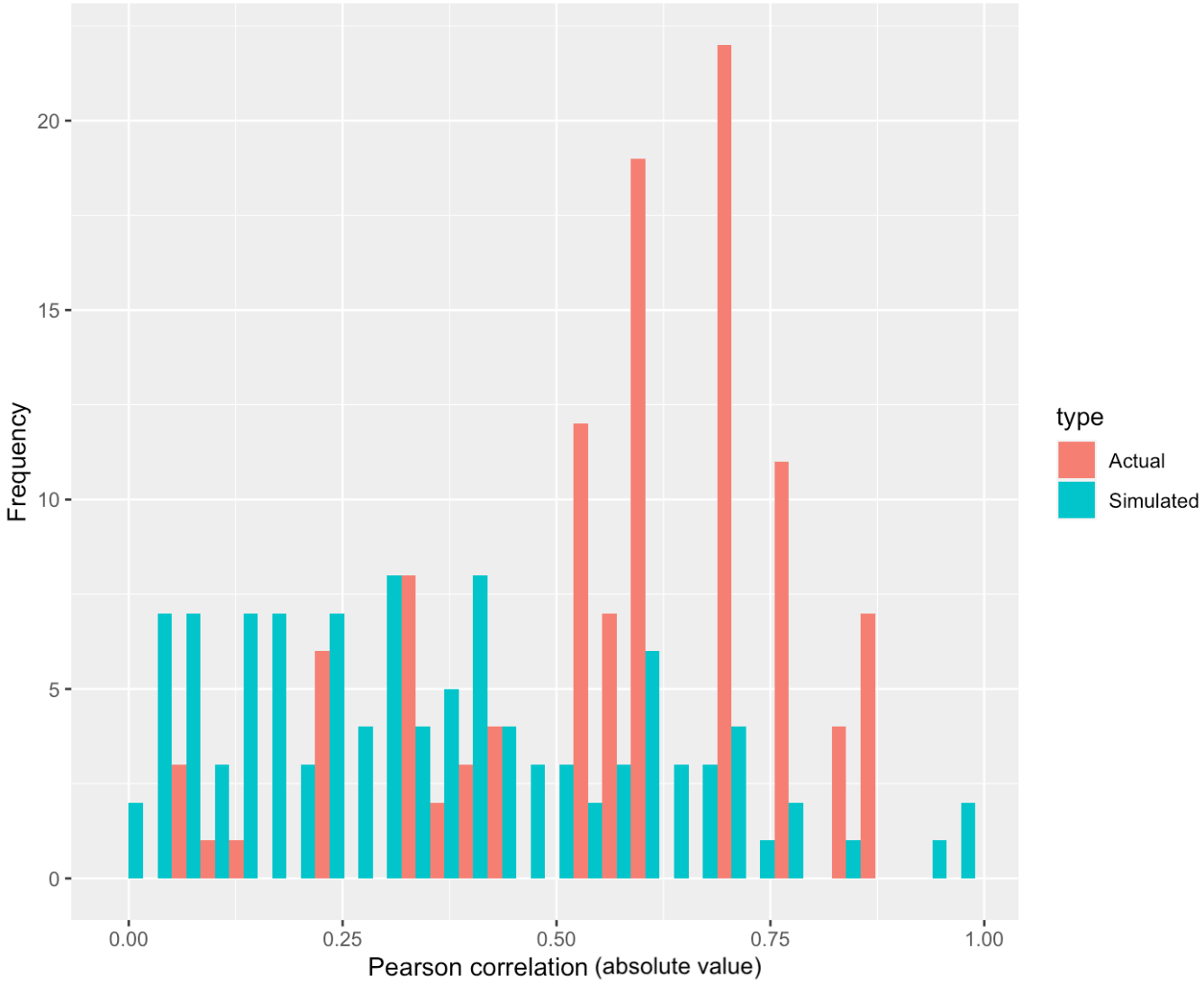

Figure S3. Simulated Pearson correlations between gaussian noise vectors of length 6 for the 110 iterations associated to each combination of the parameters k = [0.001, 0.005, 0.01, 0.05, 0.1, 0.5, 1, 5, 10, 50, 100] and γ = [0.001, 0.01, 0.1, 1, 10, 100, 1000, 10000, 100000, 1000000].